ASIAN JOURNAL OF PHARMACEUTICAL AND CLINICAL RESEARCH

INNOVARE ACADEMIC SCIENCES
Knowledge to Innovation

Vol 19, Issue 2, 2026

Online - 2455-3891
Print - 0974-2441

Research Article

SYNTHESIS AND EVALUATION OF ANTITUBERCULAR ACTIVITY OF 1, 3, 4-OXADIAZOLE DERIVATIVES

NAMITHA KN, VELMURUGAN V*

Department of Pharmaceutical Chemistry, SRM College of Pharmacy, SRM Institute of Science and Technology, Kattankulathur, Tamil Nadu, India.

***Corresponding author: Velmurugan V; Email: velmuruv@srmist.edu.in**

Received: 04 August 2025, Revised and Accepted: 05 December 2025

ABSTRACT

Objective: The present study aimed to design, synthesize, and evaluate two novel series of 1,3,4-oxadiazole derivatives for their antitubercular activity against *Mycobacterium tuberculosis* H37Rv, supported by molecular docking and absorption, bio-distribution, metabolism, and excretion (ADME) predictions to identify potential lead molecules.

Methods: Two series of oxadiazole derivatives2-(3-phenoxybenzylideneamino)-5-(4-substituted phenyl)-1,3,4-oxadiazoles (Series 1a-1e) and N-[5-(4-substituted phenyl)-1,3,4-oxadiazol-2-yl]-5-oxo-1-phenylpyrrolidine-3-carboxamides (Series2a-2e)were synthesized and structurally confirmed using melting point analysis, Ultraviolet-Visible, IR, ^{1}H-NMR, and mass spectrometry. Antitubercular activity was assessed using the Alamar Blue Assay against *M. tuberculosis* H37Rv, with isoniazid (INH) as the standard. Molecular docking studies were performed against Enoyl-Acyl Carrier Protein Reductase (InhA), and ADME properties were predicted using an online computational server.

Results: Docking studies indicated strong binding affinities for compounds 1e and 2c, with docking scores of −10.7 and −10.5, respectively, suggesting potent interaction with InhA. ADME analysis showed that most derivatives possessed favorable drug-like properties, although compounds 1c and 1d exhibited Lipinski's rule violations. Biological screening revealed that compound 2b demonstrated the most significant antitubercular activity, with a minimum inhibitory concentration of 1.6 µg/mL compared with the standard drug INH.

Conclusion: The synthesized oxadiazole derivatives exhibited moderate to strong antitubercular activity, supported by promising docking scores and acceptable ADME properties. These findings identify derivatives such as 2b as potential leads for further optimization and development of novel antitubercular agents.

Keywords: Oxadiazole, Antitubercular activity, Pyrrolidine carboxamide.

 DOI: http://dx.doi.org/10.22159/ajpcr.2026v19i2.56395. Journal homepage: https://innovareacademics.in/journals/index.php/ajpcr

INTRODUCTION

Tuberculosis is also known as TB, it is a highly contagious disease caused by tubercular bacilli, i.e., *Mycobacterium tuberculosis,* which selectively affects the lungs. In general, it is transmitted through airborne particles when the TB patients cough, sneeze, or spit. Approximately 1.25 million people died due to TB in 2023, as per the latest report from WHO.TB has resurfaced as the leading cause of death worldwide by surpassing COVID-19 in the same year. TB stands as a major global health concern, particularly among individuals living with HIV, and is a significant contributor to the growing problem of antimicrobial resistance. Irrespective of age, TB is prevalent in every region of the world. In 2023 almost 10.8 million people developed TB which included 6 million male population, 1.3 million children and 3.6 million women, and 1.3 million children. Despite its global burden, TB is both preventable and curable through timely diagnosis and appropriate medical treatment. The WHO's fact sheet dated March 14, 2025, stated that TB is projected to be a leading cause of morbidity and death worldwide [1].

A serious concern for global health is the rise of drug-resistant TB. Even though rifampicin, isoniazid (INH), and ethambutol have long been essential first-line antibiotics in TB treatment plans, resistance to these medications has grown in frequency and is a serious public health issue in many areas. Compared to drug-susceptible TB, multidrug-resistant TB is linked to longer treatment durations, higher healthcare expenses, and noticeably worse clinical outcomes. Treating multidrug-resistant TB is very difficult for individuals who also have HIV, as they are more susceptible to severe illness and treatment failure. The up-rise prevalence of drug-resistant TB highlights the pressing need for the creation of new anti-tubercular medications and creative treatment approaches.

2,5-disubstituted-1,3,4-oxadiazole derivatives are reported to elicit a wide spectrum of biological activities. The activities also include various literatures, such as antimicrobial [2,3], anti-viral, plant growth regulatory activity [4], Anti-tubercular [5], and anti-HIV activity [6]. As per various literature, 2,5-disubstituted oxadiazole analogues demonstrated significant antimicrobial, anti-mycobacterial, and anti-inflammatory properties [7-14]. This motivated us to design and synthesize a congeneric series of oxadiazole derivatives bearing an aryl-N-substituted carboxamidoethylthio side chain, to evaluate their antibacterial and antitubercular activities. The development of aryl-substituted 2,5-disubstituted oxadiazoles targeting *M. tuberculosis* H37Rv is both timely and scientifically relevant, given the pressing need for new therapeutic agents against drug-resistant TB strains. Notably, the stability of aryl-substituted oxadiazole derivatives has been well-documented and is generally superior to that of their alkyl-substituted counterparts. This enhanced stability is largely attributed to the electron-withdrawing nature of aryl groups, which contributes to the structural integrity and chemical resilience of the oxadiazole ring system.

In silico studies, including molecular docking and dynamic simulations, have played a crucial role in elucidating the interactions between the synthesized compounds and target proteins of *M. tuberculosis.* These computational investigations revealed that aryl-substituted

1,3,4-oxadiazoles exhibit strong binding affinities toward the active sites of key bacterial enzymes, potentially disrupting their function. Such insights provide valuable guidance for the rationalization of anti-tubercular drug synthesis. He *et al*., 2006 demonstrated Pyrrolidine Carboxamides as a Novel Class of Inhibitors of Enoyl Acyl Carrier Protein Reductase (InhA) from *M. tuberculosis*. The potency of the lead compound was improved over 160-fold by subsequent optimization through iterative microtiter library synthesis followed by *in situ* activity screening without purification [15].

An effective strategy is mandatory to curb the multidrug resistant TB and early detection is important to identify drug-resistant TB cases [16]. Recently developed rapid molecular diagnostic methods offer a powerful means for the early detection of resistant TB [17]. However, a comprehensive understanding of the genetic determinants responsible for drug-resistant TB with respect to geographic regions is necessary to optimise the use of existing diagnostic technologies and to inform the development of novel approaches. Moreover, such genetic insights can support national TB control programs in designing targeted and effective intervention strategies.

Extensive research demonstrated that point mutations at *rpoB* gene, which is responsible for rifampicin-resistant cases [18]. These mutations lead to structural changes in the rifampicin binding site, thereby significantly reducing the drug's efficacy and multidrug resistance. The mutation on katG is associated with INH drug resistance. Research has demonstrated that approximately 70% of 1NH-resistant Mtb isolates harbor mutations at this locus [19].

The mutation in the inhA operon leads to overexpression of the InhA enzyme, essential for mycolic acid synthesis which is an important component in *M. tuberculosis*. This overexpression reduces the efficacy of INH, requiring higher drug concentrations to effectively inhibit the enzyme, thus conferring resistance [20]. Additionally, the genetic mutations responsible for resistance to rifampicin and INH exhibit significant geographic variability, which can influence the effectiveness of molecular diagnostic techniques and treatment strategies [21-23]. Moreover, bridging both oxadiazole and pyrrolidine carboxamide may be a wise approach to design an effective anti-tubercular drug.

In response to these challenges, the current work aimed to synthesize and evaluate oxadiazole derivatives and oxadiazole clubbed pyrrolidine carboxamide derivatives as potential antitubercular agents.

EXPERIMENTAL

Methods

Chemicals

All chemicals and reagents used in this study were of analytical grade. Semicarbazide hydrochloride, sodium acetate (anhydrous), glacial acetic acid, ethanol, and bromine were procured from Sigma Aldrich and Loba Chemie Pvt. Ltd. (Mumbai, India). Substituted benzaldehydes and 3-phenoxybenzaldehyde were purchased from Spectrochem Pvt. Ltd. (Mumbai, India) and SRL Pvt. Ltd. (Mumbai, India). All solvents used were of analytical grade and were obtained from SRL India.

Instruments

The melting points of synthesized derivatives were checked by the open capillary method and uncorrected. The λ max was scanned by ultraviolet (UV)-visible spectrophotometer (T60, Lab India). Infrared (IR) spectra were recorded in a Shimadzu IR spectrophotometer using the KBr (Potassium Bromide) disc method. ^{1}HNMR spectra were recorded on a 300 MHz Bruker NMR spectrometer using the solvent dimethyl sulfoxide (DMSO-d*6*) as solvent. Molecular weight of the compound was determined by WATERS SBD mass spectrophotometer. The completion of the reaction was monitored by TLC, and the spots were visualized by UV lamp.

Scheme of synthesis

Two novel series of oxadiazole derivatives were synthesized using established methodologies, as depicted in Schemes 1 and 2.

Scheme 1

- Step 1: Synthesis of semi-carbazone
  0.1 mol of sodium acetate and 0.01 mol of semicarbazide hydrochloride were dissolved in distilled water. To this aqueous solution, 0.02 mole of substituted benzaldehyde in 15 mL of alcohol was gradually added with constant stirring. The precipitate thus obtained was filtered with vaccum pump, dried, and the crude material was recrystallized from ethanol. Melting point 213–215°C.
- Step 2: Synthesis of 4-substituted 2-amino oxadiazole
  0.05 moles of semi-carbazone, 0.073 moles of anhydrous sodium acetate, and 75 mL of acetic acid were mixed to form a slurry. After that, 0.016 mol of bromine dissolved in 5 mL of glacial acetic acid was added dropwise with constant stirring. After 2 h of stirring, the mixture was submerged in ice water. The resultant precipitate was filtered, washed with water, and air dried. The crude compound was recrystallized from ethanol and has a melting point between 238 and 240°C. All other derivatives were made using the same procedure.
- Step 3: Synthesis of 2-(3-phenoxy benzylidene amino)-5-(4-substituted phenyl) oxadiazole (1a-1e)

In 30 mL of ethanol and 1 mL of glacial acetic acid, 0.05 mol of 2-amino-5-substituted oxadiazole derivatives were dissolved. 3-Phenoxy benzaldehyde (0.05 mole) was added to the reaction mixture and refluxed for 6 h. After the reaction was over, the reaction mixture was poured into crushed ice with continuous stirring. The obtained product was filtered, washed with ice water, air dried, followed by recrystallization from aqs ethanol.

The variation in yields between compounds 1a and 1b can be attributed to the nature of their substituents. The phenolic –OH group in compound 1a increases polarity, promotes strong hydrogen bonding, and may participate in minor side reactions, leading to lower isolated yield. In contrast, compound 1b bears an electron-donating–NH_2 group that enhances the reaction rate and reduces purification losses, resulting in a comparatively higher yield.

Scheme2

- Step 1: synthesis of 4-substituted -2-amino phenyl oxadiazole by step1 mentioned in scheme 1
- Step 2: Synthesis of 5-oxo-N1 phenyl pyrrolidin-3-carboxylic acid
  200 mL of water, 0.1 mol of itaconic acid, and 0.1 mol of aniline were combined, and the mixture was refluxed for an hour. The reaction mixture was cooled, and the obtained precipitate was dissolved in dilute NaOH, followed by acidification with dilute HCl. The resultant precipitate was recrystallized from boiling water and obtained as needle shape-crystal. The melting point was determined at 246–248°C.
- Step 3: Synthesis N-(5-(4-substituted phenyl) oxadiazol-2-yl)-5-oxo-1- phenylpyrrolidine-3-carboxamide
  0.01 mol of pyrrolidin-3-carboxylic acid and 0.01 mol of oxadiazole derivatives were dissolved in 60 mL of dry DMF. 0.005 mol of DIEA, 0.002 mol of HBTU were added to the above reaction mixture and stirred for 5 h at RT. The brine solution was employed to quench the reaction, and ethyl acetate (3×50 mL) was used to extract the final product. After washing with 1N HCl, the mixed ethyl acetate layers were saturated with sodium bicarbonate. The combined organic layer was dried over anhydrous Na_2SO_4 and filtered. The resulting organic phase was subjected to reduced-pressure distillation to yield the final product. A dichloromethane-methanol mixture was used to recrystallize the resultant product.

Molecular docking studies

It was carried out using Auto dock vina software 1.2.0 to evaluate the binding energy between protein and ligands. The protein Enoyl acyl

carrier protein reductase (InhA) was downloaded from protein data bank website with PDBID: 1BVR. The protein was prepared by standard protocol, such as removing co-crystallized ligand and water molecules, followed by the addition of polar hydrogen and Kollman charges [24]. For ligand preparation, the 3D structures of the compounds were generated and energy-minimized using the MM method. Gasteiger charges were then added to the ligands. These steps ensured that both the receptor and ligands were in optimal conformations for docking simulations. Finally, the standard drug INH and the synthesized ligands were docked to the InhA enzyme to assess their binding affinities.

Swiss absorption, bio distribution, metabolism, and excretion (ADME) analysis

The pharmacokinetic properties, such as drug ADME, are critical determinants of their efficacy and safety. To evaluate these properties, we assessed the ten synthesized compounds using the Swiss ADME tool. This in silico approach estimates drug-likeness characteristics based on widely recognized pharmacokinetic metrics, including the extended Lipinski's rule of five (RO5) [25].

According to the rule of five criteria, an oral medication must not break more than one of the following guidelines: molecular weight <500; intestinal absorption-related logP and logS ≤5; membrane permeability-related HBA and HBD ≤10 and ≤5, respectively; PSA ≤140 Å. All of the molecules that were examined at 1 hour showed good drug-likeness qualities, with all of the values falling within the limits of RO5, indicating that these derivatives' oral bioavailability would be high (Table 1).

Anti-tubercular activity

The Anti-tubercular activity was carried out against *M. tuberculosis* H37Rv (MTCC 300), which was procured from MTCC in Chandigarh, India. The generated analogues were screened using the MABA method, as described in the previous literature [26]. Alamar blue is an indicator generally used to check cell growth and viability. It is blue in color in its oxidized form and changes to pink when it is reduced. A common first-line anti-tubercular medication, INH, was used as a positive control in the bio-evaluation. A distinct 96-well white plate was filled with 190 µL of *M. tuberculosis* culture. The quantities of the test chemicals, which were dissolved in DMSO, ranged from 100 µg/mL to 0.19 µg/mL. The microplates were incubated for 5 days at 37°C with 5% CO_2. After that, 15 µL Alamar blue dye was added to each microplate and incubated for another 12 h with the similar conditions. After the incubation period, the fluorescence intensity was measured at 549 nm and 519 nm as excitation and emission wavelengths. The lowest concentration at which the colour change stopped was considered the Minimum Inhibitory Concentration (MIC) [27]. All test compounds were dissolved in DMSO, and the final DMSO concentration in each well was maintained at 2 µL, a level that did not interfere with mycobacterial growth. A solvent control, containing the same concentration of DMSO but without the test compound, was included to confirm that the observed inhibitory effects were attributable to the compounds and not to DMSO itself.

RESULTS AND DISCUSSION

Chemistry

Based on Schemes 1 and 2, two series of oxadiazole derivatives were synthesized. In Scheme 1, sodium acetate was used as a catalyst when semicarbazide hydrochloride and substituted aryl aldehydes reacted. The intermediate phenylsemicarbazide formed was subsequently cyclized to yield 2-amino-5-phenyl-oxadiazole in the presence of bromine in glacial acetic acid. The final products (1a-1e) were synthesized by reacting the oxadiazole amine with 3-phenoxybenzaldehyde in the presence of glacial acetic acid (Fig. 1). Compounds 2a through 2e were synthesized according to Scheme 2. At the first step, N^1-phenylpyrrolidin-3-carboxylic acid was prepared, and then reacted with 2-amino-4-substituted phenyl oxadiazole in the presence of HBTU and DIEA (Fig. 2). The yield of the compounds varied because of the influence of steric and electronic effects. The final compounds were characterized by MP, UV, FT-IR, ^{1}H-NMR, and Mass spectra. Figs. 3-6 display the IR and ^{1}H-NMR spectra of compounds 1a and 2a.

2-(3-phenoxy benzylidene amino)-5-(4-hydroxy phenyl) oxadiazole (1a)

Colorless solid, yield 52.10%,MF: $C_{21}H_{15}N_3O_3$melting point 250–252°C, UV(MeOH): λmax 302 nm; IR (KBr, cm^{-1}): 1628(C=N), 3254(OH), 1026(C-O-C), 1116(C=C Aromatic); ^{1}H-NMR (300MHz, δ ppm) 7.34,7.57,7.60,7.77,8.80, 8.03(13H, Ar H), 8.83(C=C-H), Mass m/z (ESI+):357(M^{+1}).

2-(3-phenoxy benzylidene amino)-5-(4-aminophenyl) oxadiazole (1b)

Yellow solid, MF: $C_{21}H_{16}N_4O_2$yield 67.21%, melting point 256–258°C, UV(MeOH): λmax 292 nm; IR (KBr, cm^{-1}): 1583(C=N), 3267(NH), 1074 (C-O-C), 1018 C=C Aromatic); ^{1}H-NMR(300MHz,δ ppm) 7.22, 7.31,7.33,7.66,7.69(13H, Ar H), 8.23(C=C-H),Mass m/z (ESI+):356(M^{+1}).

2-(3-phenoxy benzylidene amino)-5-(4-ethyl phenyl) oxadiazole (1c)

Off-white solid, yield 64.16%, MF: $C_{23}H_{19}N_3O_2$melting point 280–282°C, UV(MeOH): λmax 298 nm; IR(KBr, cm^{-1}):1504(C=N), 2787,2644 (CH_2 CH_3), 1074 (C-O-C), 1018 C=C Aromatic); 1H-NMR(300MHz,δ ppm) 7.22,7.31,7.34,7.67,7.69(13H, Ar H), 8.47 (C=C-H), 2.35, 3.85(CH_2, CH_3) Mass m/z (ESI+):369(M^{+1}).

2-(3-phenoxy benzylidene amino)-5-(4-bromo phenyl) oxadiazole (1d)

Off-white solid, MF: $C_{21}H_{14}BrN_3O_{2;}$ yield; 53.06%, melting point 288–290°C, UV(MeOH):λmax 304 nm; IR(KBr, cm^{-1}):1504(C=N), 1078 (C-O-C), 1020(C=C Aromatic), 747 (C-Br); ^{1}H-NMR(300MHz,δ ppm) 7.06,7.09,7.16,7.71,7.74(13H, Ar H), 8.23 (C=C-H);Mass m/z (ESI+):420 (M^{+1}).

2-(3-phenoxy benzylidene amino)-5-(4-carboxy phenyl) oxadiazole(1e)

Off-white solid, MF: $C_{22}H_{15}N_3O_{4;}$ yield; 66%, melting point 245–247°C, UV(MeOH): λmax 328 nm; IR(KBr, cm^{-1}):1508(C=N), 1078 (C-O-C), 1020(C=C Aromatic), 1672 (C=O of COOH); 1H-NMR(300MHz,δ ppm) 7.57,7.65,7.78,7.81,7.99,8.02,8.27,8.30,8.34(13H, Ar H), 8.57 (C=C-H), Mass m/z (ESI+):385 (M^{+1}).

Table 1: Lipinski's parameter

Comp code	Log p	Molecular weight	No. of H donor	No. of H acceptors	No of non-rotatable bounds	No of violations
1a	4.10	357.36	1	6	5	0
1b	3.97	356.38	1	5	5	0
1c	5.14	369.42	0	5	6	1
1d	5.12	420.26	0	5	5	1
1e	4.07	385.37	1	7	6	0
2a	2.64	363.37	2	7	4	0
2b	1.27	314.15	3	8	4	0
2c	3.11	336.22	1	7	5	0
2d	3.01	320.74	1	7	4	0
2e	1.62	346.66	2	9	6	0

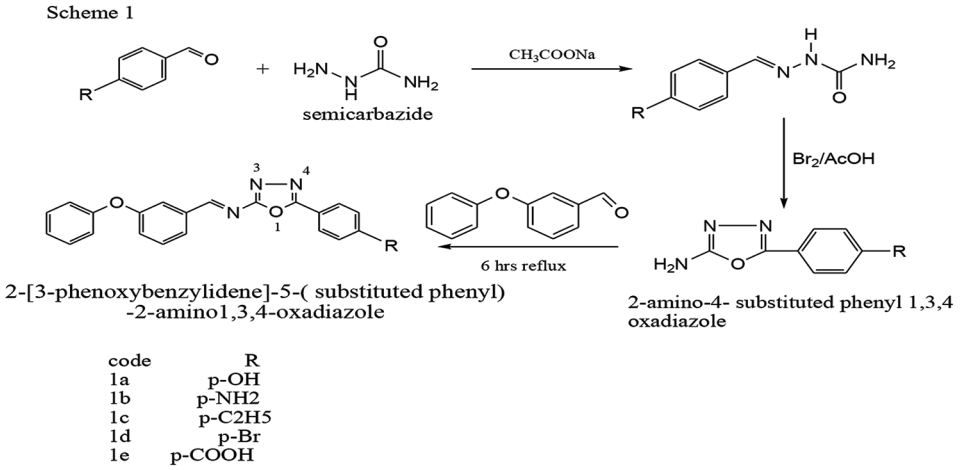

Fig. 1: Scheme of synthesis of oxadiazole derivatives

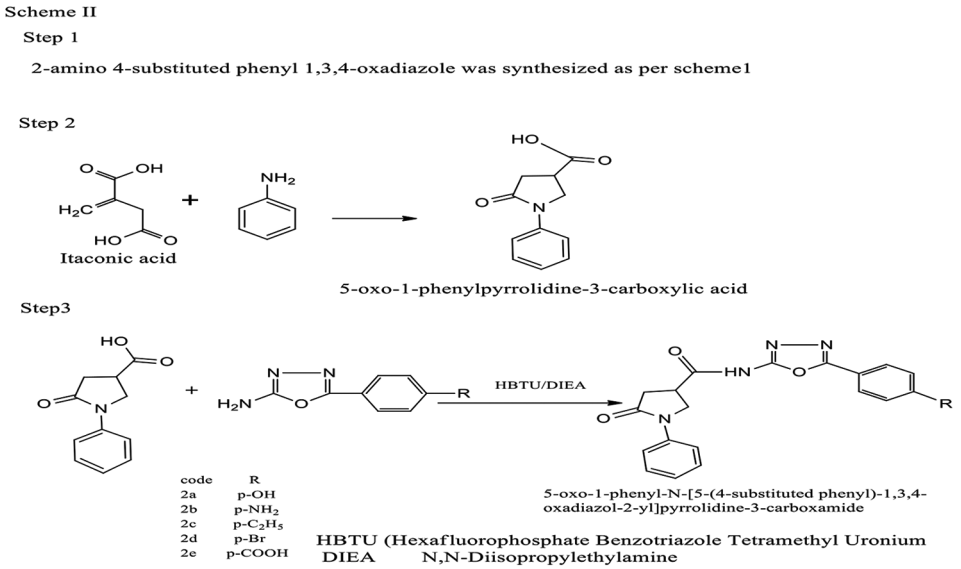

Fig. 2: Scheme of synthesis of oxadiazole derivatives

5-(4-hydroxy phenyl) -2- [N¹ phenyl -5-oxo pyrrolidin-3- carboxamido] 1, 3, 4 oxadiazole (2a)

Off-white solid, yield; 60%, MF $C_{20}H_{18}N_4O_4$,melting point 235–237°C, UV(MeOH): λmax 274 nm; IR(KBr, cm^{-1}): 3483 (N-H), 1712 (pyrrolidinyl C=O), 1616 (amide C=O), 1579 (C=N), 1078 C-O-C; 1H-NMR(300MHz,δ ppm) δ7.28, 7.29,7.37, 7.38,7.39, 7.58, 7.61 7.64, 7.68 (m,9H,Ar-H),9.42 δ (1H, NH), 2.76 δ,3.36 δ (4H, CH_2×2), 3.61 δ (1H, CH)., m/z (ESI+):364 (M^{+1}).

5-(4-amino phenyl) -2- [N¹ phenyl -5-oxo pyrrolidin-3- carboxamido] 1, 3, 4 oxadiazole (2b)

Off-white solid, yield; 60%, melting point 268–270°C, UV(MeOH): λmax 298 nm; IR(KBr, cm^{-1}): 3452 (N-H), 1700 (pyrrolidinyl C=O), 3188 (Ar-C-H), 1444.73 (Ring C=C), 1662 (amide C=O), 1612 (C=N), 1248 C-O-C; 1H-NMR(300MHz,δ ppm) δ7.28,7.27,7.32,7.38,7.49,7.58,7.61,7.68 (m,9H,Ar-H),9.16 δ (1H, NH), 2.45 δ,4.36 δ (4H, CH_2×2), 3.30 δ (1H, CH), MF $C_{20}H_{17}N_5O_3$, m/z (ESI+):364 (M^{+1}).

5-(4-ethyl phenyl) -2- [N¹ phenyl -5-oxo pyrrolidin-3- carboxamido] 1, 3, 4 oxadiazole (2c)

Off-white solid, yield; 57 %, melting point 277–279°C, UV(MeOH): λmax 295 nm; IR(KBr, cm^{-1}): 3449 (N-H), 1706 (pyrrolidinyl C=O), 3188 (Ar-C-H), 2960.42 (methyl CH stretch), 1444.73 (Ring C=C), 1706 (amide C=O), 1622 (C=N), 1242(C-O-C); 1H-NMR(300MHz,δ ppm) δ7.28,7.29,7.32,7.36,7.48,7.49, 7.58, 7.84, (m,9H,Ar-H),9.42 δ (1H, NH), 2.53 δ,2.78 δ (4H, CH_2×2), 3.30 δ (1H, CH), 2.86,3.68δ (5H, CH_2CH_3); Mass MF $C_{21}H_{20}N_4O_3$ m/z (ESI+):376 (M^{+1}).

5-(4-bromo phenyl) -2- [N¹ phenyl -5-oxo pyrrolidin-3- carboxamido] 1, 3, 4 oxadiazole (2d)

Light yellow solid, yield; 64 %, melting point 240–242°C, UV(MeOH): λmax 307 nm; IR(KBr, cm^{-1}): 3481 (N-H), 1697 (pyrrolidinyl C=O), 3190 (Ar-C-H), 1437 (Ring C=C), 1606 (amide C=O), 1579 (C=N), 1247(C-O-C); ^{1}H-NMR(300MHz,δ ppm) δ7.27,7.29,7.32,7.36,7.42, 7.47, 7.93,7.95 (m,9H,Ar-H),9.32 δ (1H, NH), 2.53 δ,4.23 δ (4H, CH_2×2), 2.92δ (1H, CH); MF $C_{19}H_{15}N_4O_3Br$ m/z (ESI+):427 (M^{+1}).

5-(4-carboxy phenyl) -2- [N¹ phenyl-5-oxo pyrrolidin-3-carboxamido] 1, 3, 4 oxadiazole (2e)

Off-white solid, yield;70%,mp 212–214°C, UV(MeOH): λ_{max} 347 nm; IR(KBr, cm^{-1}): 3460 (N-H), 1705 (pyrrolidinyl C=O), 3113 (Ar-C-H), 1464 (Ring C=C), 1627 (amide C=O), 1577 (C=N), 1242(C-O-C); ^{1}H-NMR(300MHz,δ ppm) δ7.37,7.40, 7.48, 7.52,7.57, 7.62,8.00, 8.01, 8.06, 8.55 (m,9H,Ar-H), 9.13 (1H, NH), 2.23 δ,4.23 δ (4H, CH_2×2), 2.93 (1H, CH); MF $C_{20}H_{16}N_4O_5$, m/z (ESI+):392 (M^{+1}).

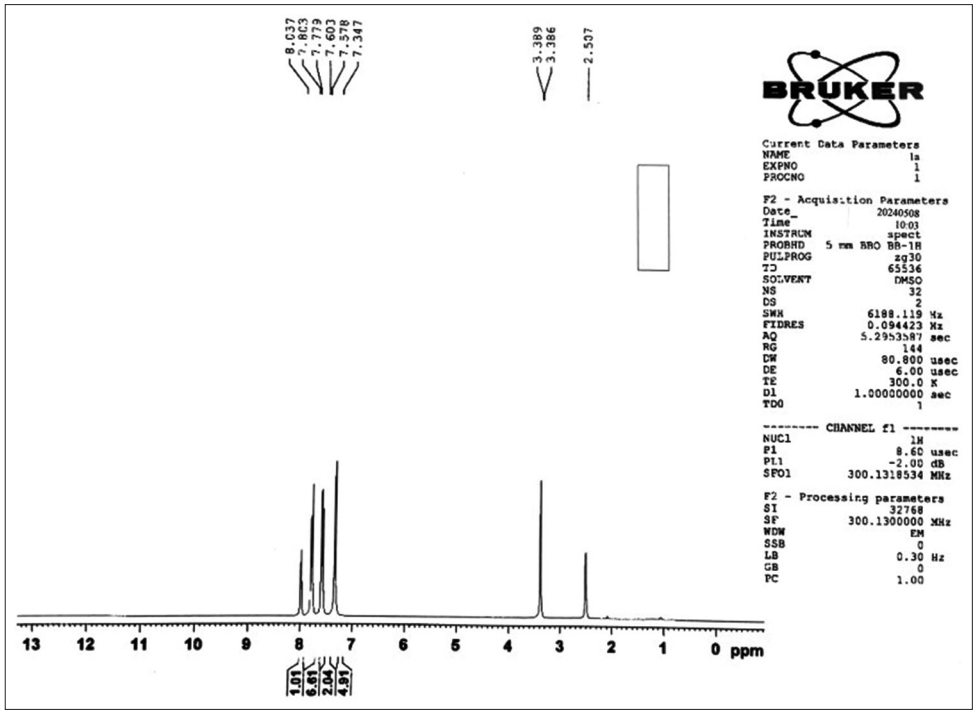

Fig. 3: ^{1}H NMR spectrum of compound 1a

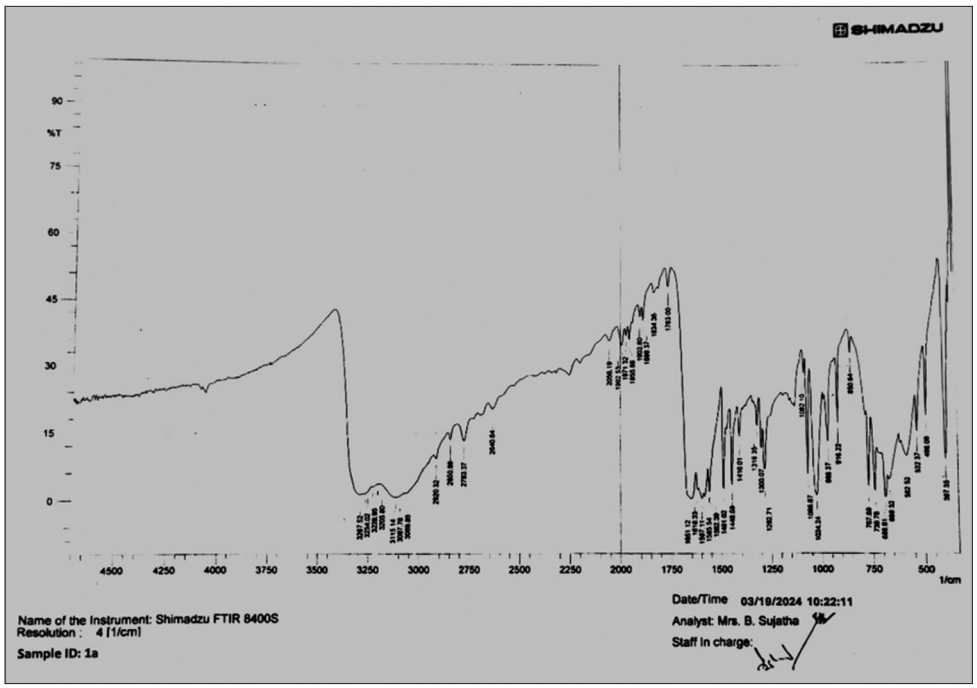

Fig. 4: FTIR spectrum of compound 1a

Molecular docking

In a recent study, molecular docking analyses were performed using the X-ray crystallographic structure of InhA (PDB ID: 1BVR) to determine the binding affinities of synthesized oxadiazole derivatives. Compounds 1e and 2c demonstrated greater binding affinities than INH, which displayed a ΔG of −5.8 kcal/mol, according to the docking data, with binding affinities of −10.7 and −10.5 kcal/mol, respectively. These findings suggest that compounds 1e and 2c may act as potent direct inhibitors of InhA (Table 2). The native ligand was re-docked with the protein 7NH5, and the RMSD was given (Table 3). The screened compounds showed a possible interaction with InhA active sites, as depicted in Figs. 7 and 8, and the interaction of the ligand with a particular amino acid is presented in Table 4. The enhanced binding affinities of these compounds are likely due to favorable interactions within the InhA active site, including hydrogen and hydrophobic interactions with key amino acid residues. Such interactions are crucial for the stabilization of the inhibitor within the enzyme's active site, thereby effectively blocking the enzyme's function.

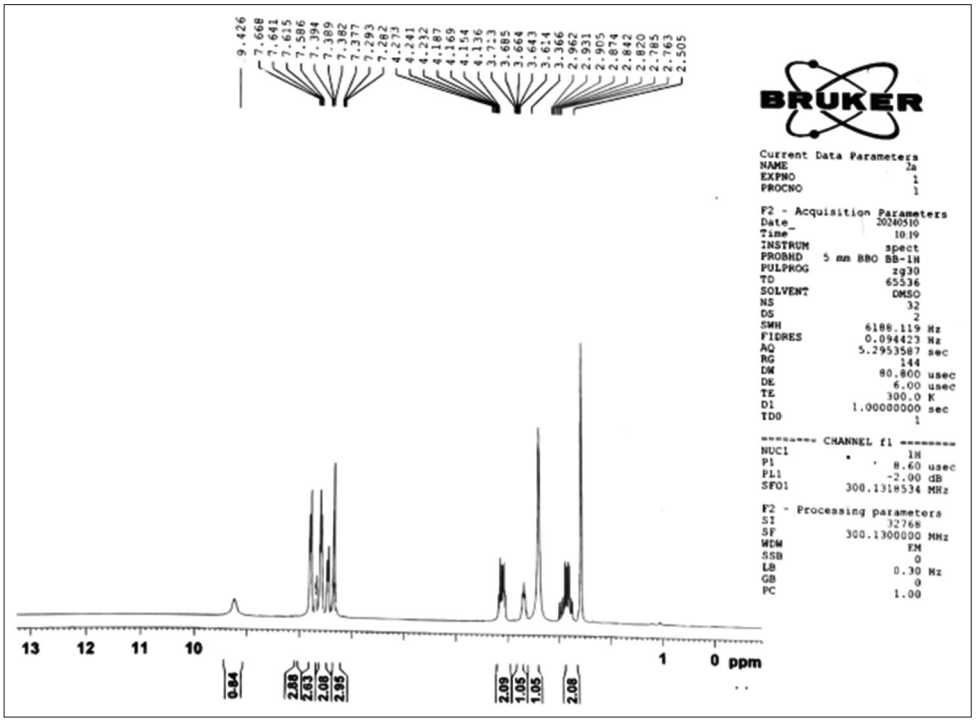

Fig. 5: ^{1}H NMR spectrum of compound 2a

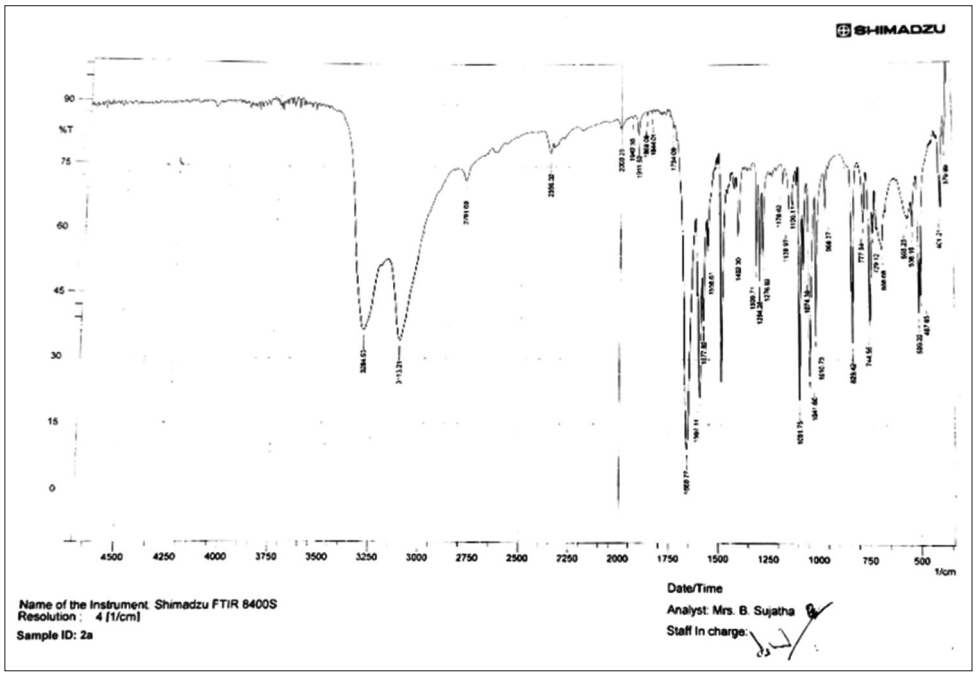

Fig. 6: FTIR spectrum of compound 2a

The pyrrolidine carboxamide series (2a-2e) generally shows stronger antitubercular activity than the diaryl ether series (1a-1e), despite both groups exhibiting similar docking scores around −10 kcal/mol. Compound 2b, which displays the lowest MIC (1.6 µg/mL), also maintains a favorable docking score, suggesting that its strong hydrogen-bonding and polar interactions translate effectively into biological potency. In contrast, compounds such as 1a-1e show weak activity (MIC 50 µg/mL) even though their docking scores are comparable, indicating that binding affinity alone does not predict *in vitro* efficacy for this scaffold. Overall, the data suggest that both binding interactions and scaffold-specific physicochemical properties influence the relationship between docking energy and antitubercular activity.

Swiss ADME

To determine the drug-likeness of the synthesized oxadiazole derivatives, Lipinski's Rule of Five, a commonly used guideline in medicinal chemistry for predicting the oral bioavailability of compounds, was applied. The following criteria must not be broken by an oral active medication, under this rule: Molecular weight <500 Daltons, octanol-water partition coefficient (LogP) ≤5, and

a maximum of 5 HBD and 10 HBA hydrogen bond donors and acceptors.

In the current study, all synthesized compounds, except for 1c and 1d, obeyed Lipinski's criteria. The molecular weights of synthesized molecules ranged from 356 to 427 Daltons, and other physicochemical properties such as LogP, HBD, and HBA values were within the acceptable limits (Table 1). The exceptions, compounds 1c and 1d, likely exceeded a few of these parameters, which may affect their oral bioavailability. These findings suggest that most of the synthesized oxadiazole derivatives possess favorable drug-like properties, making them promising candidates for the design of antitubercular drugs.

Table 2: Docking score of synthesized compounds

Compound code	Binding energy (Δkcal/mol)
1a	−10
1b	−9.9
1c	−10.3
1d	−10.3
1e	−10.7
2a	−10.3
2b	−10.3
2c	−10.5
2d	−10.3
2e	−10.3
Isoniazid	−5.8

Table 3: Validation of docking by native ligands re-docking with RMSD

PDB ID (1BVR)		
Compound	**Binding score (kcal/mol)**	**RMSD**
Native ligand nicotinamide-adenine-dinucleotide	−10.0	1.3

Table 4: Key binding interactions for compounds 1a-1e and 2a-2e

Compound	π–π stacking	Hydrophobic interactions	Hydrogen bonds
1a	Phe94	Ile120, Val65, Ile21, Ser20, Gly14, Gln66	Asp64
1b	Phe41	Val65, Ile122, Ile16, Ser20, Thr196, Gly14	Ile21
1c	Phe44, Phe49	Ile95, Ile122, Ile94, Thr196, Gly192, Ser20, Ile21	Ser20, Ile21
1d	Phe149, Phe4	Val65Ile95Ile122Met147Ile16	Gly14, Ser20
1e	Phe4	Ile194, Ile95, Ile122, Met199, Ser20, Ile16	Ile21, Gly192
2a	Phe41	Ile122, Val65, Ile16, Met147, Ile21	Asp64, Ser94
2b	Phe41	Ile95, Val65, Ser20, Ile16	Ser94, Ile21, Asp64
2c	Phe41	Ile95, Ile16, Ile122, Met147, Val65	Ser94, Gly14
2d	Phe149	Ile95, Ile122, Val65, Ile16, Gly96	Ser94, Gly14
2e	Phe44	Ile95, Ile16, Val65, Ile21, Gln66	Asp64, Ser94, Gly14

Anti-tubercular activity

Out of every synthetic molecule, derivative 2b exhibited a noteworthy MIC Value of 1.6 µg/mL. The MIC value for all of the compounds synthesized from scheme 1, or 1a-1e, was 50 µg/mL. 2-((3-phenoxybenzylidene) amino)-5-(4-substituted phenyl) oxadiazole was the outcome of research. N-(5-(4-substuituted phenyl)-1,3,4-oxadiazol-2-yl)-5-oxo-1-phenylpyrrolidine carboxamide exhibited notable anti-tubercular action, but 1, 3, 4-oxadiazole (1a-1e) derivatives did not. -3-carboxamide (2a-2e) had demonstrated notable anti-tubercular properties. The MIC value for compound 2b, for instance, was 1.6 µg/mL. However, because the MIC value was 0.4 µg/mL, all of the activity data were below that of the standard drug INH (Table 5 and Fig. 9).

INH was used as a standard drug control and provided a reliable benchmark for validating the assay, as its MIC consistently confirmed the accuracy of the experimental conditions. Its inclusion ensured that the biological screening results were comparable to established antitubercular activity standards.

SAR

A comparison of the diaryl ether series (1a-1e) and the pyrrolidine carboxamide series (2a-2e) reveals a striking scaffold-dependent difference in antibacterial activity. The flexible diaryl ether analogues are uniformly weak, with all members displaying MIC values of 50 µg/mL regardless of electronic or steric substitution. In contrast, the conformationally constrained pyrrolidine carboxamide scaffold supports clear SAR trends, with electron-donating and hydrogen-bond-donating substituents markedly enhancing potency. The most active compound, the para-amino analogue 2b, achieves an MIC of 1.6 µg/mL, demonstrating the importance of favorable polar interactions in this series. Overall, the comparison highlights that scaffold rigidity and hydrogen-bond donor capacity are critical determinants of antibacterial potency, whereas substituent effects are effectively masked in the more flexible diaryl ether framework.

Swiss ADME analysis

The compound 2a-2e series had shown better binding affinities than 1a-1e series. This docking score prediction was also reflected in anti-tubercular activity since the second series of compounds demonstrated significantly more activity than the former. This result was also supported by the Lipinski rule finding. As shown in Table 1, it was found that the second series of compounds had no violation of the Lipinski rule, whereas the first series had violations which are 1d and 1e. The compounds 2a-2e, molecular weight lesser than 1a to 1e series, and lower log p-values. Among all, compound 2b had shown promising anti-tubercular activity, which may be due to low log p-value, low molecular weight, and a greater number of H donors and acceptors.

Table 5: Anti-tubercular activity data

Compound code	MIC (µg/mL)
1a	50
1b	50
1c	50
1d	50
1e	50
2a	12.5
2b	1.6
2c	50
2d	25
2e	12.5
INH	0.4

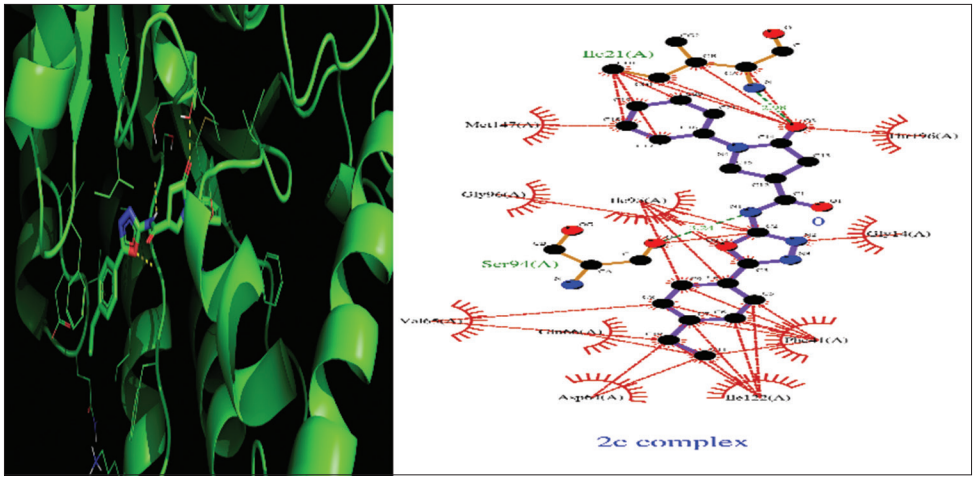

Fig. 7: Docking interaction of ligand 2c with InhA and associated amino acids

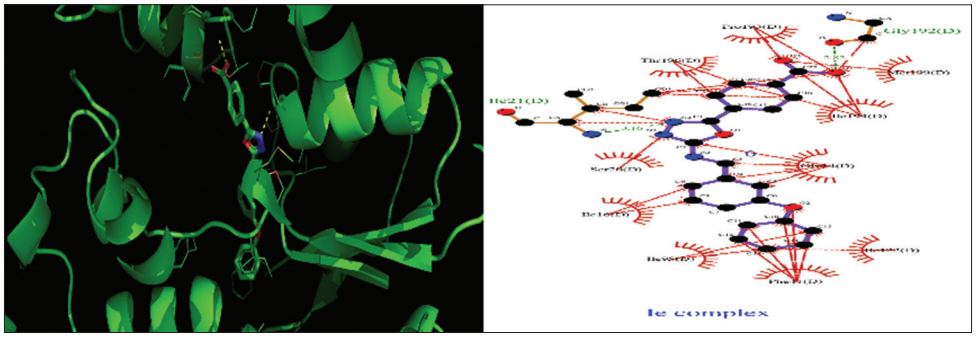

Fig. 8: Docking interaction of ligand 1e with InhA and associated amino acid

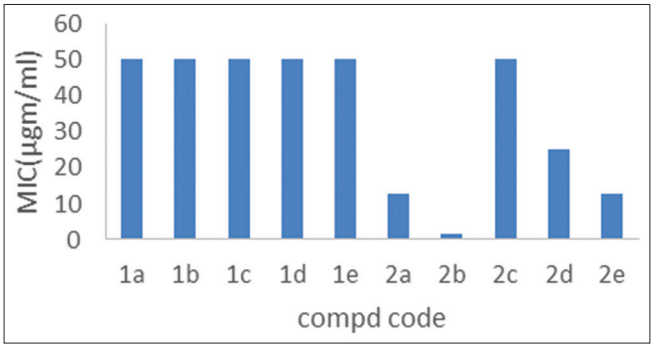

Fig. 9: Comparison of anti-tubercular activity

CONCLUSION

Two series of oxadiazole derivatives were synthesized, and their anti tubercular activity was assessed. Most of the derivatives were synthesized with high purity and in good yields. Compounds 2b's addition of electron-donating groups produced outstanding antitubercular action. According to docking analysis, the oxadiazole derivatives might generate important bound and non-bonded interactions with the InhA active site. The promising *in silico* findings, corroborated by *in vitro* antitubercular activity, lay a robust foundation for advancing structure-based drug design aimed at developing potent and selective anti-tubercular agents. Notably, compound 2b, an oxadiazole derivative fused with a pyrrolidine ring, has demonstrated remarkable anti-tubercular efficacy and a high docking score, underscoring its potential as a lead compound for further optimization.

ACKNOWLEDGMENTS

We would like to thank SRM University's Research and Development Council for providing the facilities needed to carry out this research project.

AUTHOR CONTRIBUTIONS

Velmurugan Vadivel: Conceptualization of research, methodology, and supervised the entire project. NAMITHA KN: Executed the work, writing and editing the manuscript.

CONFLICT OF INTEREST

The authors declare no conflict of interest.

FUNDING

Nil.

REFERENCES

1. WHO. Report on Tuberculosis. W.H.O. Fact Sheet at 14th March; 2025.
2. Kadi AA, El-Brollosy NR, Al-Deeb OA, Habib EE, Ibrahim TM, El-Emam AA. Synthesis, antimicrobial and anti-inflammatory activities of 1,3,4-oxadiazole derivatives. Eur J Med Chem. 2010;45(12):5006-11. doi: 10.1016/j.ejmech.2010.08.020.
3. Khazi IM, Koti RS, Mahajanshetti CS, Somani RR. Synthesis and antimicrobial activity of some 2-(N-substituted carboxamidomethyl/ethylthio)-5-(2′-thienyl)-1,3,4-oxadiazoles. Indian J Heterocycl Chem. 2003 Jul 1;13(1):87-8.
4. Edward LH. U.S. Patent. Chem Abstract, 95. 1981;4(259):25078f.
5. Liberman D, Rist N. Congress Intern Biochemistry Resumés Communs. 3rd Vol. 51. Chemistry, Brussels; 1957. p. 14137f.

6. Bondock S, Fadaly W, Metwally MA. Synthesis and antimicrobial activity of some new 1,3,4-oxadiazole derivatives. Eur J Med Chem. 2010;45(9):3692-701. doi: 10.1016/j.ejmech.2010.05.062[GM3]
7. Sonar VN, Hadimani MB. Synthesis of pyrazolylindoles and oxadiazolylindoles-their anti-inflammatory activity. Indian J Heterocycl Chem. 1998 Oct 1;8:125-8.
8. Donawade DS, Raghu AV, Gadaginamath GS. Synthesis and antimicrobial activity of some new 1-substituted-3-pyrrolyl aminocarbonyl/oxadiazolyl/triazolyl/5-methoxy-2-methylindoles and benz [g] indoles. Indian J Chem B. 2006 Mar 1;45(3):689.
9. Küçükgüzel SG, Oruç EE, Rollas S, Sahin F, Ozbek A. Synthesis, characterisation and biological activity of novel 4-thiazolidinones, 1,3,4-oxadiazoles and some related compounds. Eur J Med Chem. 2002 Mar;37(3):197-206. doi: 10.1016/s0223-5234(01)01326-5, PMID 11900864
10. Kučerová-Chlupáčová M. Systematic review on 1,2,3-oxadiazoles, 1,2,4-oxadiazoles, and 1,2,5-oxadiazoles in the antimycobacterial drug discovery. ChemMedChem. 2025 May 5;20(9):e202400971. doi: 10.1002/cmdc.202400971, PMID 39846226
11. Pflégr V, Stolaříková J, Karabanovich G, Maixnerová J, Pál A, Korduláková J, *et al*. 5-(3,5-dinitrophenyl)-1,3,4-oxadiazol-2-amine derivatives, their precursors, and analogues: synthesis and evaluation of novel highly potent antitubercular agent. PLOS One. 2025 May 29;20(5):e0324608. doi: 10.1371/journal.pone.0324608, PMID 40440331, PMCID PMC12121777
12. Asif M, Farhan SS. An overview on antitubercular activity profile of fluoroquinolone derivatives and their molecular hybridization. J Med Chem. 2020;3:145-53. doi: 10.26655/jmchemsci.2020.2.6
13. Jasim SF, Mustafa YF. Synthesis and antidiabetic assessment of new coumarin-disubstituted benzene conjugates: An *in silico in virto* study. J Med Chem Sci. 2022;5(6):887-99. doi: 10.26655/JMCHEMSCI.2022.6.3
14. Lihumis HS, Alameri AA, Zaooli RH. A review on recent development and biological applications of benzothiazole derivatives. Prog Chem Biochem Res. 2022;5:147-64. doi: 10.22034/pcbr.2022.330703.1214
15. He X, Alian A, Stroud R, Ortiz De Montellano PR. Pyrrolidine carboxamides as a novel class of inhibitors of enoyl acyl carrier protein reductase from *Mycobacterium tuberculosis*. J Med Chem. 2006 Oct 19;49(21):6308-23. doi: 10.1021/jm060715y, PMID 17034137, PMCID PMC2517584
16. Aye KS, Nakajima C, Yamaguchi T, Win MM, Shwe MM, Win AA, *et al*. Genotypic characterization of multi-drug-resistant *Mycobacterium tuberculosis* isolates in Myanmar. J Infect Chemother. 2016 Mar;22(3):174-9. doi: 10.1016/j.jiac.2015.12.009, PMID 26806152
17. Van Rie A, Warren R, Mshanga I, Jordaan AM, Van Der Spuy GD, Richardson M, *et al*. Analysis for a limited number of gene codons can predict drug resistance of *Mycobacterium tuberculosis* in a high-incidence community. J Clin Microbiol. 2001 Feb;39(2):636-41. doi: 10.1128/JCM.39.2.636-641.2001, PMID 11158121, PMCID PMC87790
18. Zhang Y, Vilchèze C, Jacobs WR. Mechanisms of drug resistance in *Mycobacterium tuberculosis*. In: Cole ST, Eisenach KD, McMurray DN, Jacobs WR, editors. Tuberculosis and the Tubercle *Bacillus*. Chichester: John Wiley and Sons; 2004. p. 115-40. doi: 10.1128/9781555817657.ch8
19. Unissa AN, Subbian S, Hanna LE, Selvakumar N. Overview on mechanisms of isoniazid action and resistance in *Mycobacterium tuberculosis*. Infect Genet Evol. 2016 Nov;45:474-92. doi: 10.1016/j.meegid.2016.09.004, PMID 27612406
20. Ramaswamy S, Musser JM. Molecular genetic basis of antimicrobial agent resistance in *Mycobacterium tuberculosis*: 1998 update. Tuber Lung Dis. 1998;79(1):3-29. doi: 10.1054/tuld.1998.0002, PMID 10645439
21. Spindola De Miranda S, Kritski A, Filliol I, Mabilat C, Panteix G, Drouet E. Mutations in the *rpoB* gene of rifampicin-resistant *Mycobacterium tuberculosis* strains isolated in Brazil and France. Mem Inst Oswaldo Cruz. 2001 Feb;96(2):247-50. doi: 10.1590/s0074-02762001000200019, PMID 11285505
22. Hillemann D, Kubica T, Rüsch-Gerdes S, Niemann S. Disequilibrium in distribution of resistance mutations among *Mycobacterium tuberculosis* Beijing and Non-Beijing strains isolated from patients in Germany. Antimicrob Agents Chemother. 2005 Mar;49(3):1229-31. doi: 10.1128/AAC.49.3.1229-1231.2005, PMID 15728936, PMCID PMC549281
23. Bollela VR, Namburete EI, Feliciano CS, Macheque D, Harrison LH, Caminero JA. Detection of katG and inhA mutations to guide isoniazid and ethionamide use for drug-resistant tuberculosis. Int J Tuberc Lung Dis. 2016 Aug;20(8):1099-104. doi: 10.5588/ijtld.15.0864, PMID 27393546, PMCID PMC5310937
24. Aiswariya BV, Satya MS, Satya MS. Molecular docking and ADMET studies of benzotriazole derivatives tethered with isoniazid for antifungal activity. Int J Curr Pharm Res. 2022;14(4):78-80. doi: 10.22159/ijcpr.2022v14i4.2004
25. Dhawale S, Gawale S, Jadhav A, Gethe K, Raut P, Hiwarale N, *et al*. *In silico* approach targeting polyphenol as FabH inhibitor in bacterial infection. Int J Pharm Pharm Sci. 2022;14(11):25-30. doi: 10.22159/ijpps.2022v14i11.45816
26. Madriwala B, Suma BV, Jays J. Molecular docking study of hentriacontane for anticancer and antitubercular activity. Int J Chem Res. 2022 Oct;6(4):1-4. doi: 10.22159/ijcr.2022v6i4.208
27. Kachkure D, Sa D, Tapadiya G, Pawar C, Bharad J. Synthesis and evaluation of diazo-triazole hybrid as anti-tubercular agents. Int J Chem Res. 2025;9(4):34-9. doi: 10.22159/ijcr.2025v9i4.281.